

Supplementary Information

Advanced Photoelectrochemical Performance of Inverse-opal Heterostructures Fabricated using Hydrogenated ZnO and TiO₂

Zheli Wu^a, Jie Long^a, Ming Fu^{a,*}, Xiaoyu Liu^a, Jiefeng Li^a, Peixin Chu^a, Chenhui Wei^a, Yuting Zhang^a, Yijun Ning^b, Dawei He^a, Yongsheng Wang^a

^aKey Laboratory of Luminescence and Optical Information, Ministry of Education, Institute of Optoelectronic Technology, Beijing Jiaotong University, Beijing 100044, PR China

^bSchool of Optical and Electronic Information, Suzhou City University, Suzhou 215104, PR China

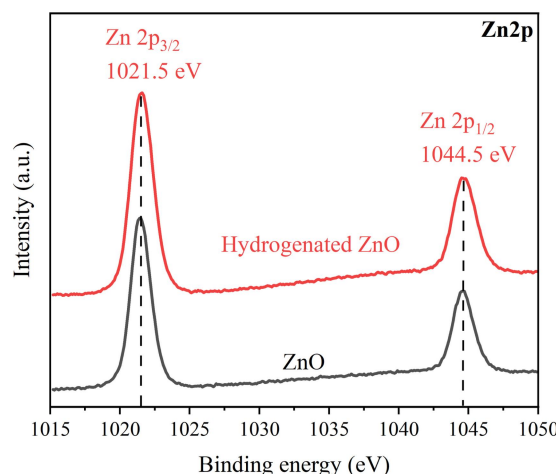


Figure S1 Zn 2p XPS spectra of ZnO IOs and H:ZnO IOs.

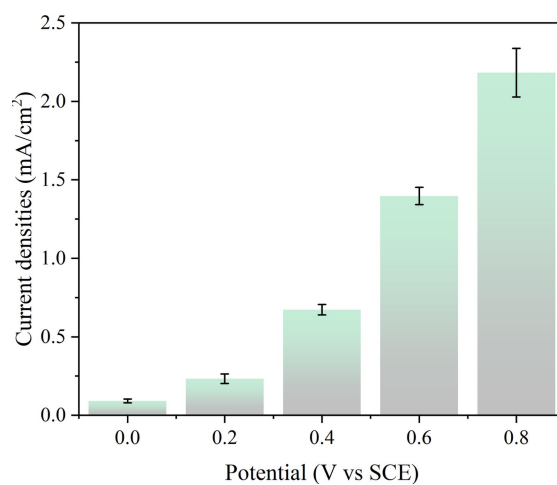


Figure S2 Current densities of 195 nm H:ZnO 350°C 3h IOs at different applied biases with error bars.

Table S1 Comparative results of the recently reported ZnO-based photoanode materials

Samples	Photocurrent densities at applied bias	Testing conditions	References
TiO ₂ nanorod	0.51 mA/cm ² at 1.23 V vs RHE	0.1 M NaOH	1
TiO ₂ nanotube	0.32 mA/cm ² at 1.23 V vs RHE	1 M KOH	2
TiO ₂ nanorod arrays	0.73 mA/cm ² at 1.23 V vs RHE	1 M Na ₂ SO ₄	3
TiO ₂ inverse opal	0.56 mA/cm ² at 1.23 V vs RHE	0.5 M Na ₂ SO ₄	4
ZnO nanorod	0.92 mA/cm ² at 1.23 V vs RHE	0.1 M KOH	5
ZnO inverse opal	0.99 mA/cm ² at 1.23 V vs RHE	0.25 M Na ₂ S/0.35 M Na ₂ SO ₃	6
ZnO nanotube	0.60 mA/cm ² at 1.23 V vs RHE	0.35 M Na ₂ S/0.25 M Na ₂ SO ₃	7
Hydrogenated ZnO nanoparticles	4.20 μA /cm ² at 0 V vs SCE	0.1 M Na ₂ SO ₄ under visible-light irradiation ($\lambda > 420$ nm)	8
Hydrogenated ZnO nanoparticles	9.50 μA /cm ² at 0 V vs SCE	0.1 M Na ₂ SO ₄ under UV-light irradiation ($\lambda = 254$ nm)	8
Hydrogenated ZnO nanorod arrays	1.00 μA /cm ² at 0.1 V vs SCE	1.0 M CH ₃ OH	9
Hydrogenated ZnO/CdS core-shell nanorod arrays	7.40 μA /cm ² at 0.5 V vs SCE	1.0 M CH ₃ OH	9
Hydrogenated ZnO nanorods	0.62 mA/cm ² at 1.6 V vs SCE	0.5 M Na ₂ SO ₄	10
Hydrogenated TiO ₂ /ZnO inverse opals	1.77 mA/cm ² at 0.6 V vs SCE	0.5 M Na ₂ SO ₄	This work

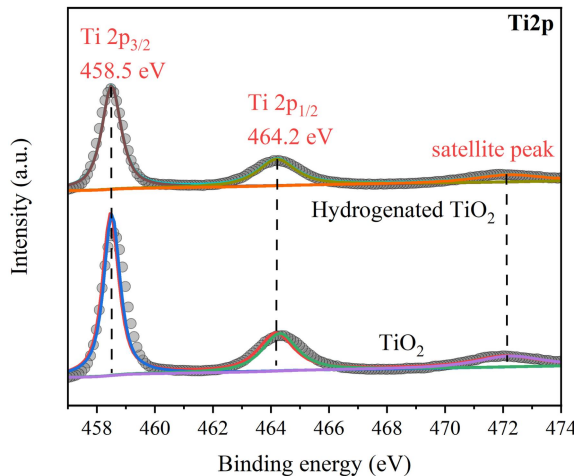


Figure S3 Ti 2p XPS spectra of TiO₂ IOs and H: TiO₂ IOs.

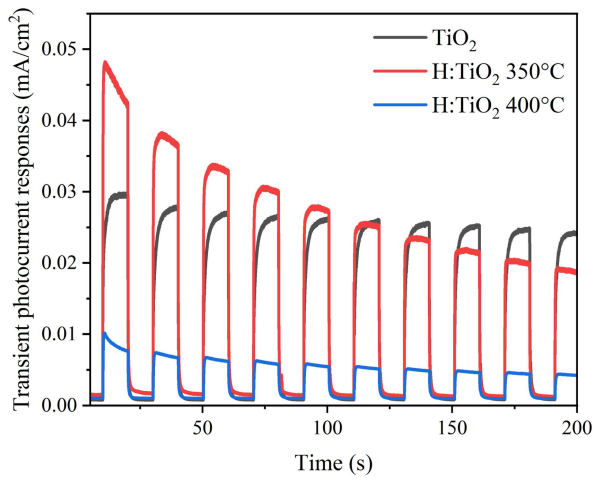


Figure S4 Transient photocurrent responses (100 mW/cm^2 , 0.6 V vs SCE) of H:TiO₂ IOs synthesized by 60 circles of ALD using 255 nm colloidal crystal templates, annealed at different temperatures for 3 hours.

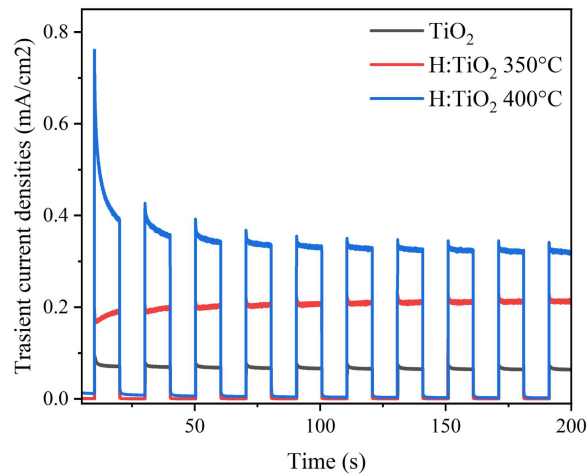


Figure S5 Transient photocurrent responses (100 mW/cm^2 , 0.6 V vs SCE) of H:TiO₂ IOs synthesized by 150 circles of ALD using 255 nm colloidal crystal templates, annealed at different temperatures for 3 hours.

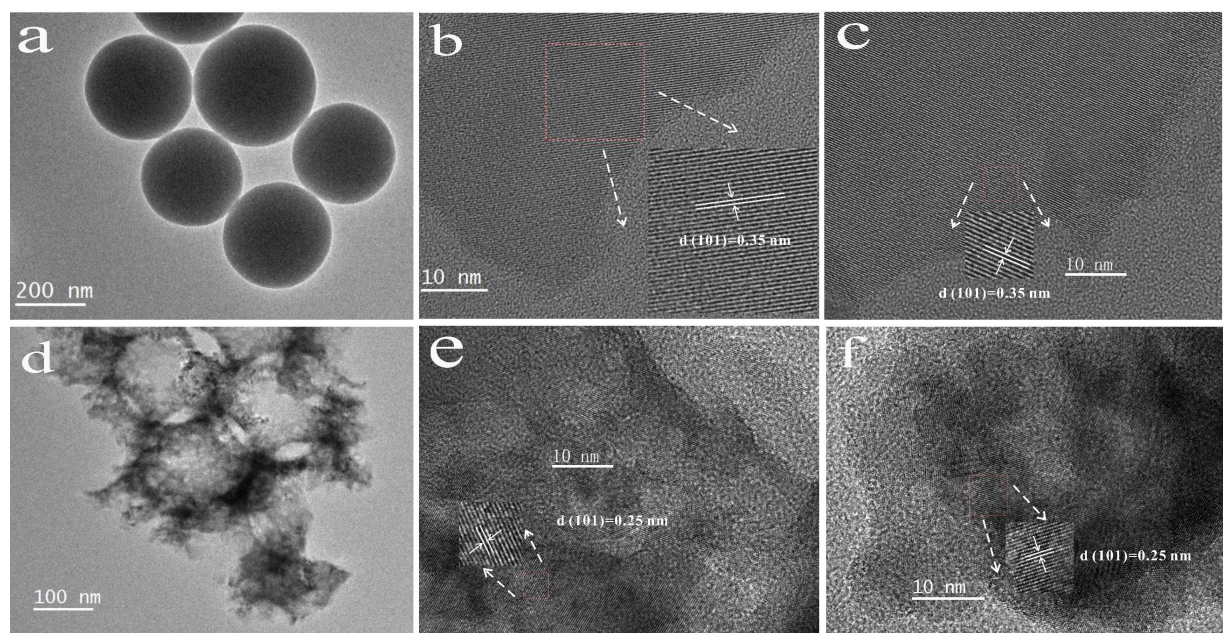


Figure S6 HRTEM images of (a), (b)TiO₂, (c)hydrogenated TiO₂, (d), (e)ZnO, and (f) hydrogenated ZnO inverse opals.

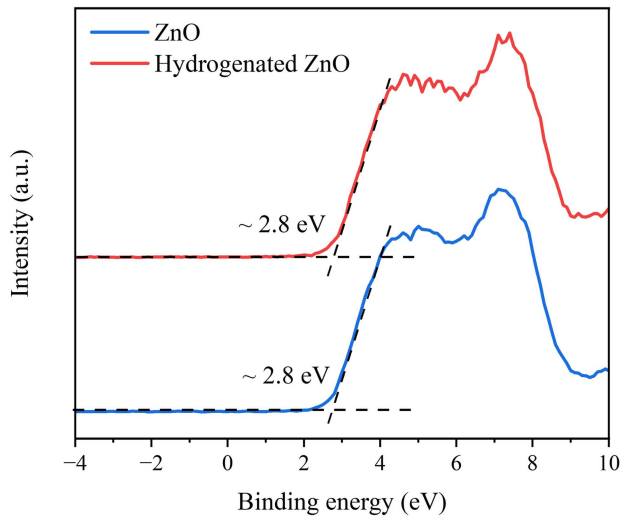


Figure S7 XPS valence band spectra of the pristine ZnO and the H:ZnO IOs.

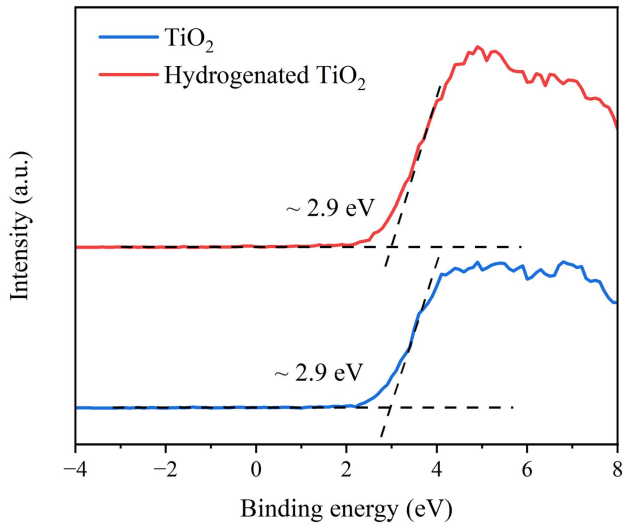


Figure S8 XPS valence band spectra of the pristine TiO_2 and the H: TiO_2 IOs.

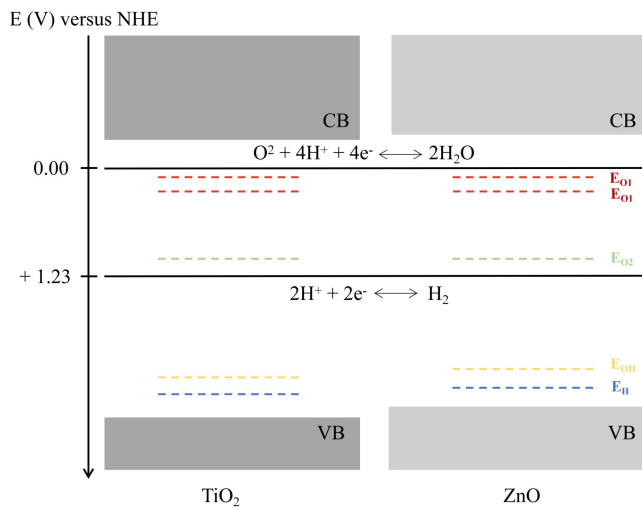


Figure S9 Simplified energy diagram of hydrogenated ZnO and hydrogenated TiO_2 . $E_{\text{O}1}$ and $E_{\text{O}2}$ are referred to the energy levels of surface oxygen vacancies and bulk oxygen vacancies, respectively. E_{OH} indicates the energy levels of surface hydroxyl group. E_{H} represents the energy levels of interstitial hydrogen.

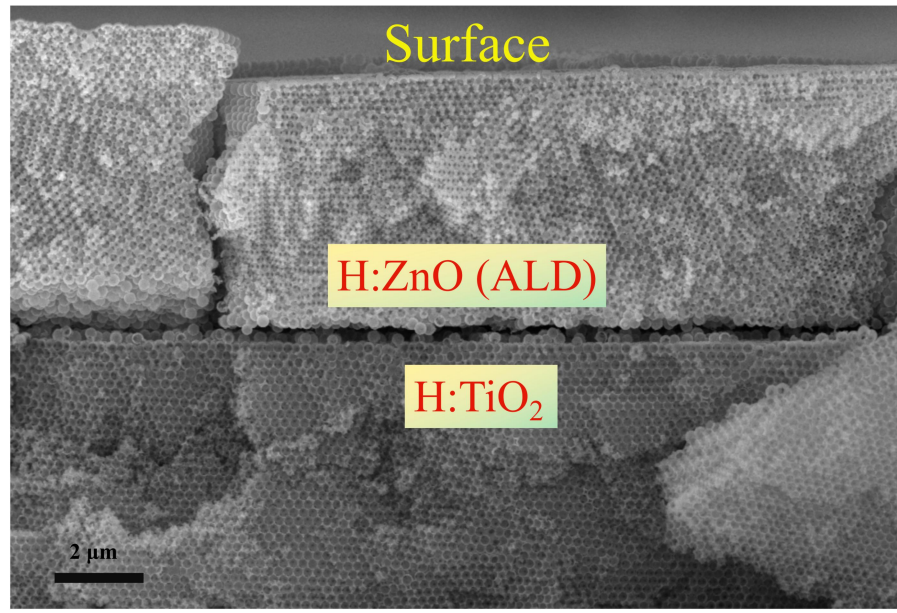


Figure S10 The cross-section SEM image of H:TiO₂/ZnO (ALD) IOs

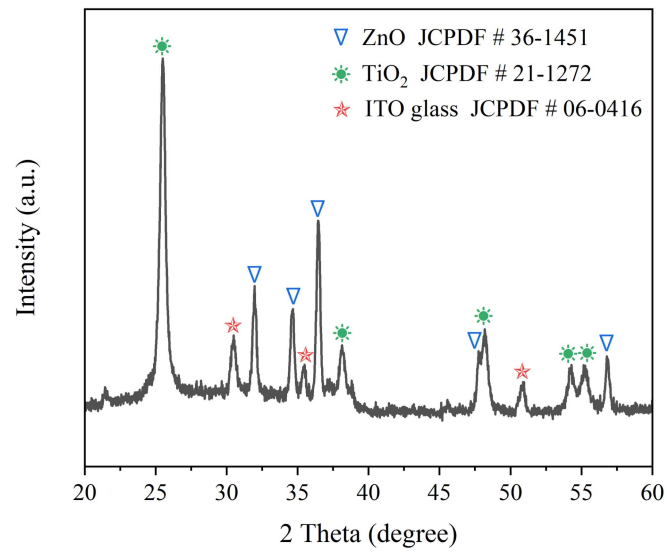


Figure S11 XRD pattern of the H:TiO₂/H:ZnO (ele) IOs

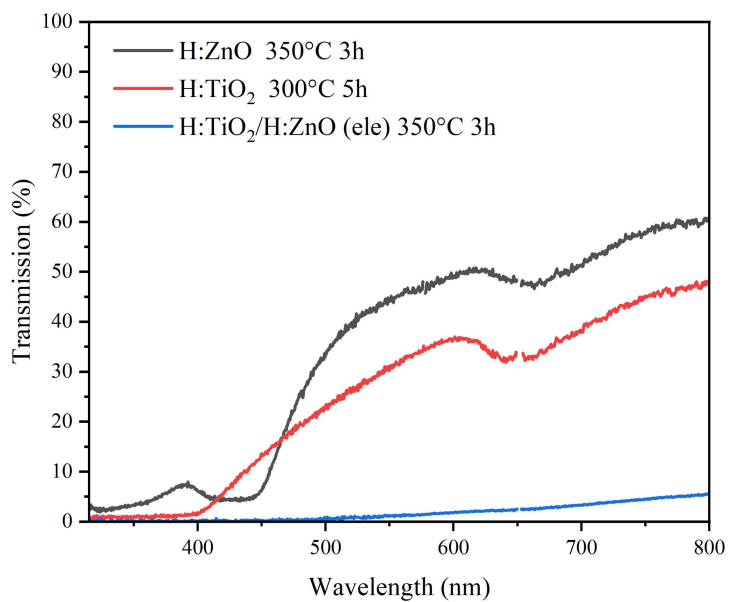


Figure S12 The transmission spectra of H:ZnO IOs, H:TiO₂ IOs, and H:TiO₂/ZnO (ele) IOs.

Notes and references

- 1 C. Chen, Y. Wei, G. Yuan, Q. Liu, R. Lu, X. Huang, Y. Cao and P. Zhu, Synergistic effect of Si doping and heat treatments enhances the photoelectrochemical water oxidation performance of TiO₂ nanorod arrays, *Adv. Funct. Mater.*, 2017, **27**, 1701575.
- 2 Y. Xu, M. A. Melia, L.-k. Tsui, J. M. Fitz-Gerald and G. Zangari, Laser-induced surface modification at anatase TiO₂ nanotube array photoanodes for photoelectrochemical water oxidation, *J. Phys. Chem. C*, 2017, **121**, 17121-17128.
- 3 M. P. Suryawanshi, U. V. Ghorpade, S. W. Shin, M. G. Gang, X. Wang, H. Park, S. H. Kang and J. H. Kim, Enhanced solar water oxidation performance of TiO₂ via band edge engineering: a tale of sulfur doping and earth-abundant CZTS nanoparticles sensitization, *ACS Catal.*, 2017, **7**, 8077-8089.
- 4 R. Boppella, S. T. Kochuveedu, H. Kim, M. J. Jeong, F. Marques Mota, J. H. Park and D. H. Kim, Plasmon-sensitized graphene/TiO₂ inverse opal nanostructures with enhanced charge collection efficiency for water splitting, *ACS Appl. Mater. Inter.*, 2017, **9**, 7075-7083.
- 5 X. Li, S. Liu, K. Fan, Z. Liu, B. Song and J. Yu, MOF - based transparent passivation layer modified ZnO nanorod arrays for enhanced photoelectrochemical water splitting, *Adv. Energy Mater.*, 2018, **8**, 1800101.
- 6 Y. Zeng, T. Yang, C. Li, A. Xie, S. Li, M. Zhang and Y. Shen, Zn_xCd_{1-x}Se nanoparticles decorated ordered mesoporous ZnO inverse opal with binder-free heterojunction interfaces for highly efficient photoelectrochemical water splitting, *Appl. Catal. B-Environ.*, 2019, **245**, 469-476.
- 7 J. Long, W. Wang, S. Fu and L. Liu, Hierarchical architectures of wrinkle-like ZnFe₂O₄ nanosheet-enwrapped ZnO nanotube arrays for remarkably photoelectrochemical water splitting to produce hydrogen, *J. Colloid Interface Sci.*, 2019, **536**, 408-413.

- 8 Y. Lv, W. Yao, X. Ma, C. Pan, R. Zong and Y. Zhu, The surface oxygen vacancy induced visible activity and enhanced UV activity of a ZnO_{1-x} photocatalyst, *Catal. Sci. Technol.*, 2013, **3**, 3136-3146.
- 9 H. Li, C. Yao, L. Meng, H. Sun, J. Huang and Q. Gong, Photoelectrochemical performance of hydrogenated ZnO/CdS core–shell nanorod arrays, *Electrochim. Acta*, 2013, **108**, 45-50.
- 10 V. Gurylev, C.-Y. Su and T.-P. Perng, Hydrogenated ZnO nanorods with defect-induced visible light-responsive photoelectrochemical performance, *Appl. Surf. Sci.*, 2017, **411**, 279-284.